Carbon nanohorns allow acceleration of osteoblast differentiation via macrophage activation.

Eri Hirata, Eijiro Miyako, Nobutaka Hanagata, Natsumi Ushijima, Norihito Sakaguchi, Julie Russier, Masako Yudasaka, Sumio Iijima, Alberto Bianco, Atsuro Yokoyama

Nanoscale

PAPER

View Article Online
View Journal | View Issue

Cite this: *Nanoscale*, 2016, **8**, 14514

Carbon nanohorns allow acceleration of osteoblast differentiation *via* macrophage activation†

Eri Hirata,*[a] Eijiro Miyako,[b] Nobutaka Hanagata,[c] Natsumi Ushijima,[d] Norihito Sakaguchi,[e] Julie Russier,[f] Masako Yudasaka,[b,g] Sumio Iijima,[g] Alberto Bianco[f] and Atsuro Yokoyama[a]

Received 4th April 2016,
Accepted 27th June 2016

DOI: 10.1039/c6nr02756c

www.rsc.org/nanoscale

Carbon nanohorns (CNHs), formed by a rolled graphene structure and terminating in a cone, are promising nanomaterials for the development of a variety of biological applications. Here we demonstrate that alkaline phosphatase activity is dramatically increased by coculture of human monocyte derived macrophages (hMDMs) and human mesenchymal stem cells (hMSCs) in the presence of CNHs. CNHs were mainly localized in the lysosome of macrophages more than in hMSCs during coculturing. At the same time, the amount of Oncostatin M (OSM) in the supernatant was also increased during incubation with CNHs. Oncostatin M (OSM) from activated macrophage has been reported to induce osteoblast differentiation and matrix mineralization through STAT3. These results suggest that the macrophages engulfed CNHs and accelerated the differentiation of mesenchymal stem cells into the osteoblast *via* OSM release. We expect that the proof-of-concept on the osteoblast differentiation capacity by CNHs will allow future studies focused on CNHs as ideal therapeutic materials for bone regeneration.

Introduction

Bone fractures, osteoarthritis, osteoporosis or bone cancers represent common and serious clinical problems. The management and reconstruction of damaged or diseased bone tissues is still an important global healthcare challenge to improve the lives of the patients in order to recover their normal functions and health.[1]

Carbon nanomaterials, such as carbon nanotubes (CNTs), graphene and carbon nanohorns (CNHs), have been studied for biomedical applications because of their unique characteristics.[2–11] Carbon nanomaterials are promising candidates for bone tissue engineering applications due to their superior cytocompatible, mechanical and electrical properties.[12–18] Some years ago we initiated a program on the applications of carbon nanomaterials for bone tissue regeneration. We have reported that CNT-coated substrates can be effective for the adhesion and differentiation of osteoblasts, while CNT-coated collagen sponges resulted in possessing a favorable biocompatibility profile with bone.[19–22] On the other hand, the impurities (*e.g.* metal catalysts and amorphous carbons) and the high aspect ratio of CNTs might lead to concerns about their safety for clinical uses.[23,24]

There is currently a great interest in creating biomedical applications using CNHs,[25–27] owing to their advantages, such as low toxicity and huge inner nanospaces for drug loading.[28,29] We previously found that CNHs promoted bone formation within a period of 2 weeks.[25] More interestingly, we observed that a high amount of CNHs was localized inside the macrophages around the newly formed bone.[25] However, the mechanism of bone formation by CNHs has not been clarified yet. Therefore, in this study, we focused our attention on the effect of macrophages loaded with CNHs on osteoblast differentiation. Several studies have reported that immune cells including monocytes and macrophages are key players in bone tissue integration with various biomaterials.[30] We hypothesized that CNHs will be able to stimulate the macrophages

[a]*Department of Oral Functional Prosthodontics, Division of Oral Functional Science, Graduate School of Dental Medicine, Hokkaido University, Kita 13, Nishi 7, Kita-ku, Sapporo 060-8586, Japan. E-mail: erieri@den.hokudai.ac.jp; Tel: +81 11706 4270*
[b]*Nanomaterials Research Institute (NMRI), National Institute of Advanced Industrial Science and Technology (AIST), Tsukuba Central 5, 1-1-1 Higashi, Tsukuba, Ibaraki 305-8565, Japan*
[c]*Nanotechnology Innovation Station, National Institute for Materials Science, 1-2-1 Sengen, Tsukuba, Ibaraki 305-0047, Japan*
[d]*Support Section for Education and Research, Graduate School of Dental Medicine, Hokkaido University, Kita 13, Nishi 7, Kita-ku, Sapporo 060-8586, Japan*
[e]*Center for Advanced Research of Energy and Materials, Faculty of Engineering, Hokkaido University, Kita 13, Nishi 8, Kita-ku, Sapporo 060-8586, Japan*
[f]*CNRS, Institut de Biologie Moléculaire et Cellulaire, Laboratoire d'Immunopathologie et Chimie Thérapeutique, 67000 Strasbourg, France*
[g]*Meijo University, Graduate School of Science and Technology, 1-501, Shiogamaguchi, Tenpaku, Nagoya, Aichi 468-8502, Japan*
†Electronic supplementary information (ESI) available. See DOI: 10.1039/c6nr02756c

for the production of osteoinductive factors such as cytokines, which are necessary for the differentiation of hMSCs into osteoblasts and the formation of new bone. Nicolaidou *et al.* reported that monocytes/macrophages cultured on human bone marrow-derived mesenchymal stem cells directly and potently induced hMSC differentiation into osteoblasts.[31] On the basis of these findings, in this study, hMDMs were cultured with hMSCs in the presence of CNHs, in order to elucidate the effect of CNHs on macrophages for the differentiation of the stem cells into osteoblasts. First, the influence and localization of CNHs into hMDMs were investigated. The increase in the amount of alkaline phosphatase (ALP) activity from coculturing hMDMs and hMSCs with CNHs was assessed. In addition, we evidenced that the expression of Oncostatin M (OSM), a multifunctional cytokine that induces osteoblast differentiation and matrix mineralization, increased in the presence of CNHs.[32] The obtained results show more accurately how CNHs can influence the formation of new bone.

Results

In order to clearly observe the cellular uptake of CNHs during the coculture of hMSCs and hMDMs, stem cells, labelled with CMPTX dye, and the macrophages were cultured with CNHs functionalized with fluorescent Alexa488-BSA (Alexa-BSA-CNHs) for 24 hours (Fig. 1). During cell culturing with increasing concentrations of CNHs, we observed that 50 μg mL^{-1} (the highest dose used) of CNHs was extensively aggregated in the culture medium. So we decided to use 5 μg mL^{-1} of CNHs for the sub-

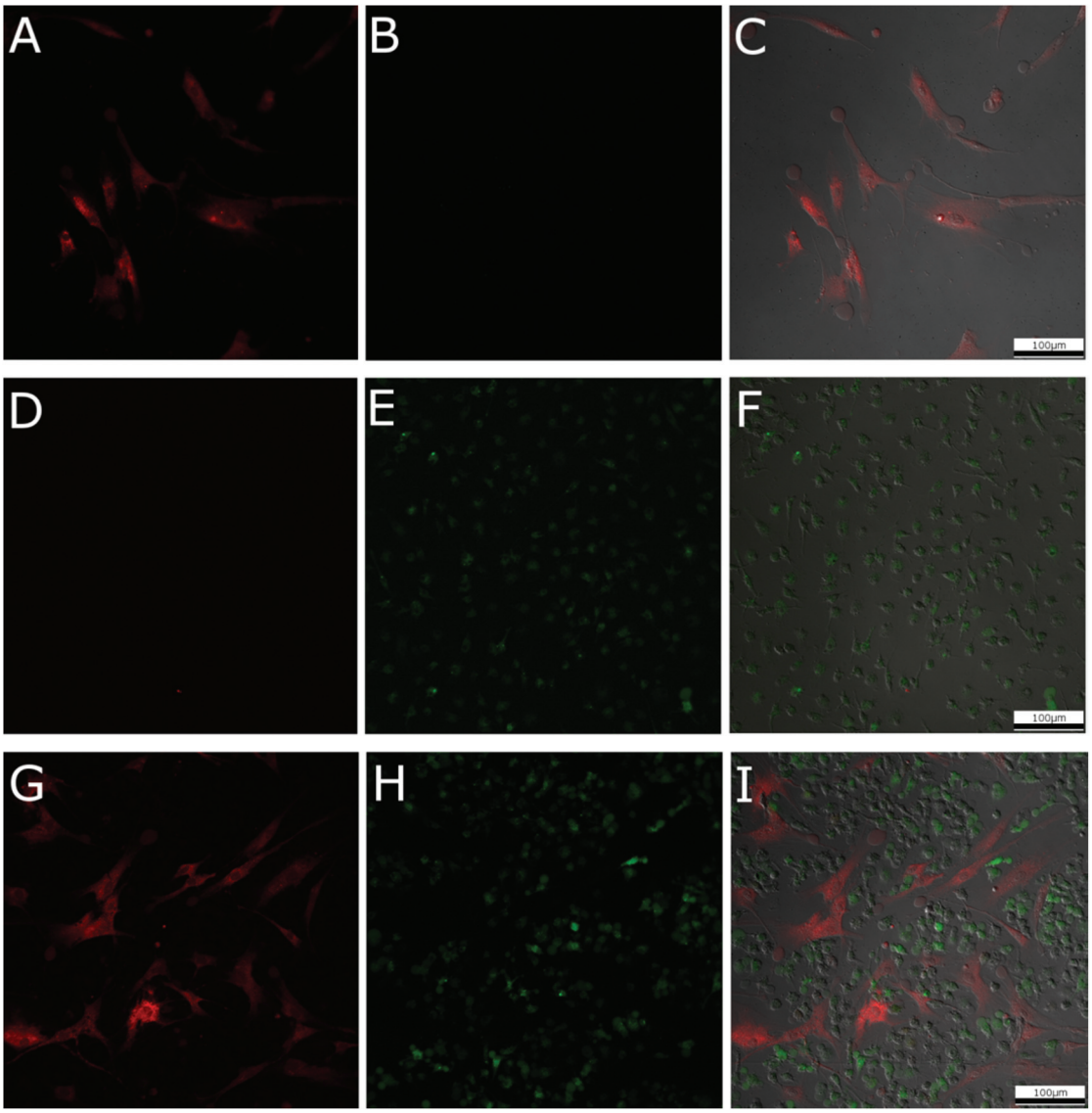

Fig. 1 Confocal laser microscopy images of Alexa-BSA-CNHs. Fluorescent (green) CNHs were added to only hMSCs (A–C), only hMDMs (D–F) and to their cocultures (G–I). hMSCs were stained with the Cell Tracker Red CMPTX dye. (A, D and G) Cells were observed with the filter for Alexa488. (B, E and H) Cells were observed with the filter for CMPTX dye. (C, F and I) Merged images.

sequent experiments. CNHs at 5 μg mL^{-1} remained well dispersed for 7 days in cell culture media. The confocal microscopy images showed that very few Alexa-BSA-CNHs were present inside the hMSCs. There were significantly low levels of fluorescence from Alexa-BSA-CNHs in these cells (Fig. 1A–C). On the other hand, most of the hMDMs were able to internalize a large number of fluorescent Alexa-BSA-CNHs (Fig. 1D–F). More interestingly, we could observe that high amounts of Alexa-BSA-CNHs were also present inside the hMDMs in comparison with hMSCs under coculturing conditions (Fig. 1G–I).

To further observe the presence of CNHs in these two types of cells, the cellular uptake behavior of CNHs after coculturing for 24 hours was analyzed by TEM (Fig. 2). Many CNHs were clearly observed in the hMDMs that were in close contact with the hMSCs (Fig. 2B). The morphology and structure of the cells were not affected compared to the control cells without CNHs (Fig. 2A). Most of the macrophages were in close contact with stem cells (Fig. 2C and D). We observed many CNHs in the cytoplasmic vesicles. In the lysosomes and the endosomes, CNHs taken up by hMDMs preserved their globular structures (Fig. 2E), similar to control CNHs (Fig. 2F). After 7 days of coculturing, CNHs mainly remained inside the hMDMs (Fig. S1†).

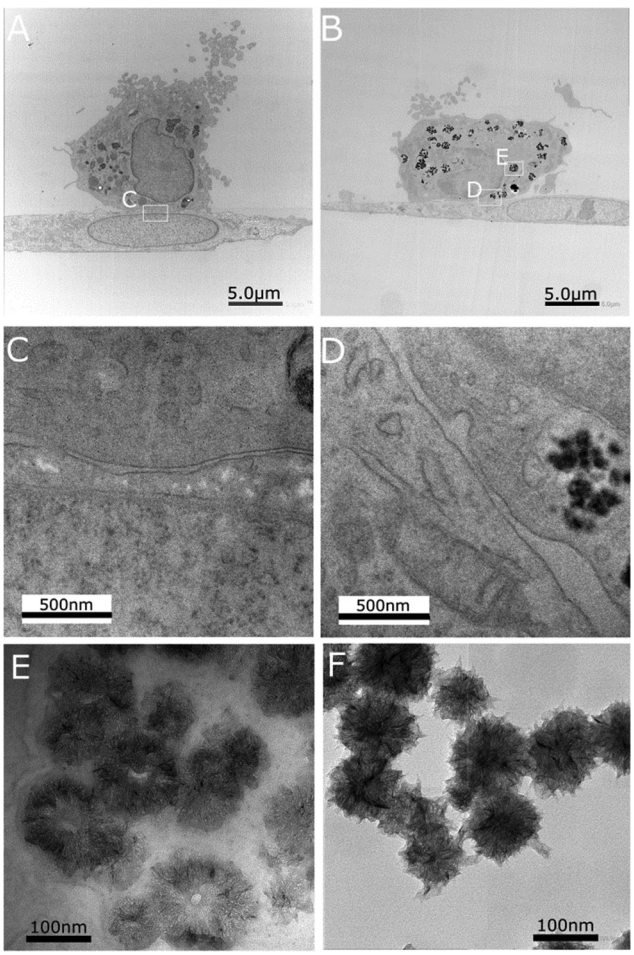

Fig. 2 TEM observations of cocultures without CNHs (A) and with CNHs (B). (C) and (D) High magnifications, corresponding to the white frames in (A) and (B), showing the tight contact between the cells. (E) High magnification corresponding to the white frame in (B) showing CNHs in a cytoplasmic vesicle. (F) Control CNHs.

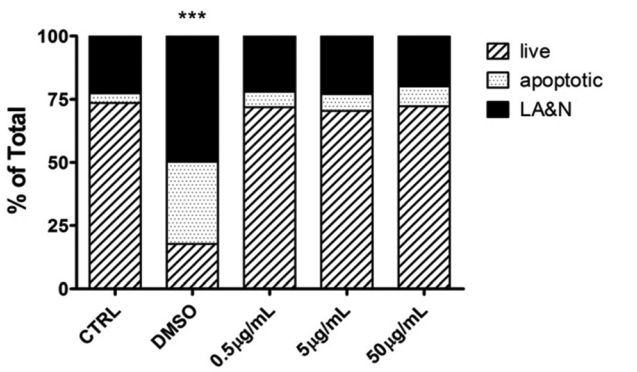

Fig. 3 Flow cytometry analysis of cellular viability of hMDMs exposed to different concentrations of CNHs. The two-way ANOVA followed by the Bonferroni's post-test was performed to determine the statistical differences *versus* control cells and to compare the three CNH samples with each other (***$p < 0.001$). LA&N: Late apoptotic and necrotic cells.

Next, hMDMs were incubated with different concentrations of CNHs (0.5, 5.0, 50 μg mL^{-1}) for 24 hours to explore the effect of CNHs on the cellular viability of human macrophages. At the end of the incubation time, the cells were stained with AnnV and PI to determine the cell viability (Fig. 3). CNHs did not cause any significant necrosis or apoptosis at any concentrations compared with the untreated cells. The quantity of CD86, a co-stimulatory molecule expressed by macrophages upon activation,[28] was not affected at the different concentrations of CNHs tested (Fig. S2†).

In order to explore cell response to CNHs by gene expression, microarray analysis was carried out after culturing hMDMs with CNHs for 24 hours. We identified 30 modified genes in hMDMs treated with CNHs. We identified 30 differentially expressed genes whose fold-change represented by the logarithmic ratio (log_2 ratio) to the expression level of the control was more than 1 (>1) and less than −1 (<−1). Of these 30 altered genes, 16 were up-regulated and 14 were down-regulated genes (Table 1). By classifying these genes into the Gene Ontology (GO) Biological Process category, we obtained 5 statistically significant ($p < 1 \times 10^{-5}$) GO terms that are related to lymphocyte migration from the CNH up-regulated genes (Table 2). On the other hand, no GO terms were obtained from the CNH down-regulated genes. The up-regulated genes classified into the lymphocyte migration related GO terms included genes that encode chemokines like CCL3, CCL4 and CXCL12 (Table 2). The expression levels of these chemokine-related genes were also analyzed by real time RT-PCR, and this analysis verified the upregulation in hMDMs treated with CNHs (Fig. 4).

ALP is one of the osteoblastic differentiation markers at the early stages. After 7 days, ALP activity was higher in the cocultured hMSCs and hMDMs both with and without CNHs compared with those of MSCs alone. Moreover ALP activity in cocultures is dramatically increased by CNHs at 5 μg mL^{-1}

Table 1 List of genes up-regulated (A) and down-regulated (B) by adding CNHs to hMDMs after for 24 hours. Fold-change is represented by the logarithmic ratio (log_2 ratio) to the expression level in control

Gene name	Systematic name	CNHs/CTRL [rep.]	Description
A			
CCL4	NM_002984	1.472	Chemokine (C–C motif) ligand 4 (CCl4), mRNA
NFATC2	NM_173091	1.405	Nuclear factor of activated T-cells, cytoplasmic, calcineurin-dependent 2 (NFATC2), transcript variant 2, mRNA
G0S2	NM_015714	1.372	G0/G1 switch 2 (G0S2), mRNA
ANKRD29	NM_173505	1.365	Ankyrin repeat domain 29 (ANKRD29), mRNA
CCL4L2	NM_001291470	1.343	Chemokine (C–C motif) ligand 4-like 2 (CCL4L2), transcript variant CCL4L2b2, mRNA
FBLN5	NM_006329	1.251	Fibulin 5 (FBLN5), mRNA
CCL3	NM_002983	1.229	Chemokine (C–C motif) ligand 3 (CCL3), mRNA
FBLIM1	NM_017556	1.167	Filamin binding LIM protein 1 (FBLIM1), transcript variant 1, mRNA
CXCL12	NM_199168	1.147	Chemokine (C–X–C motif) ligand 12 (CXCL12), transcript variant 1, mRNA
CTSZ	ENST00000503833	1.135	Cathepsin Z (source: HGNC symbol; Acc: 2547)
NAF1	NM_138386	1.119	Nuclear assembly factor 1 ribonucleoprotein (NAF1), transcript variant 1, mRNA
FN1	NM_054034	1.099	Fibronectin 1 (FN1), transcript variant 7, mRNA
P2RY1	NM_002563	1.092	Purinergic receptor P2Y, G-protein coupled, 1 (P2RY1), mRNA
PARP15	NM_001113523	1.085	Poly(AOP-ribose) polymerase family, member 15 (PARP15), transcript variant 1, mRNA
CCL3L3	NM_001001437	1.024	Chemokine (C–C motif) ligand 3-like 3 (CCL3L3), mRNA
NEURL3	NM_001285486	1.000	Neuralized E3 ubiquitin protein ligase 3 (NEURL3), transcript variant 2, mRNA
B			
IGF2BP1	NM_006548	−1.942	Insulin-like growth factor 2 mRNA binding protein 1 (IGF2BP1), transcript variant 1, mRNA
TIPARP	NM_001184717	−1.459	TCDD-inducible poly(ADP-ribose) polymerase (TIPARP), transcript variant 1, mRNA
SULF2	NM_018837	−1.291	Sulfatase 2 (SULF2), transcript variant 1, mRNA
CNR2	NM_001841	−1.240	Cannabinoid receptor 2 (macrophage) (CNR2), mRNA
CYP1B1	NM_000104	−1.151	Cytochrome P450, family 1, subfamily B, polypeptide 1 (CYP1B1), mRNA
XYLT1	NM_022166	−1.139	Xylosyltransferase I (XYLT1), mRNA
FRY	NM_023037	−1.130	Furry homolog (Drosophila) (FRY), mRNA
CTTNBP2	NM_033427	−1.106	Cortactin binding protein 2 (CTTNBP2), mRNA
LOC100128288	NR_024447	−1.077	Uncharacterized LOC100128288 (LOC100128288), long non-coding RNA
LOC100127886	AF090938	−1.070	Clone HQ0628 PRO0628 mRNA, complete cds.
LINC00926	NR_024433	−1.067	Long intergenic non-protein coding RNA 926 (LINC00926), long non-coding RNA
CLEC10A	NM_182906	−1.030	C-type lectin domain family 10, member A (CLEC10A), transcript variant 1, mRNA
S100B	NM_006272	−1.007	S100 calcium binding protein B (S100B), mRNA
PRRT1	NM_030651	−1.002	Proline-rich transmembrane protein 1 (PRRT1), mRNA

Table 2 The gene ontology of different sets of genes from the microarray over-represented in macrophages cultured with CNHs *versus* macrophages cultured without CNHs

GO ID	GO term	*P*-value	Genes			
GO:2000403	Positive regulation of lymphocyte migration	4.65×10^{-7}	CCL3	CCL4	CXCL12	
GO:2000401	Regulation of lymphocyte migration	1.37×10^{-6}	CCL3	CCL4	CXCL12	
GO:2000503	Positive regulation of natural killer cell chemotaxis	5.12×10^{-6}	CCL3	CCL4		
GO:0072676	Lymphocyte migration	6.26×10^{-6}	CCL3	CCL4	CXCL12	
GO:0043270	Positive regulation of ion transport	8.20×10^{-6}	CCL3	CCL4	CXCL12	P2RY1

(Fig. 5A). CNHs further increased the ALP activity of cocultures after 14 days, while the ALP activity of hMSCs cocultured with hMDM did not change in the absence of CNHs (Fig. 5B).

Several studies have reported that monocytes and macrophages directly regulate the osteogenic differentiation of MSCs through a mechanism that involves cell contact, leading to the production of OSM by the monocytes.[31,33] In this study, OSM levels in supernatants from hMSCs cocultured with hMDM treated with and without CNHs were measured in order to investigate whether OSM is one of the soluble factors increased by CNHs during coculturing. The amount of OSM in the supernatant with CNHs was 3 times higher than that of the control experiment without CNHs (Fig. 6A). To measure how much the OSM in the coculturing medium with CNHs affects the induction of ALP, an OSM-neutralized antibody was added to hMSC and hMDM cocultures at increasing concentrations (2, 20 and 200 ng ml^{-1}) with and without CNHs. ALP activity was quantified after 7 days. The addition of the OSM-neutralizing antibody in the cocultured hMSCs and hMDMs with CNHs prevented the ALP induction (Fig. 6B).

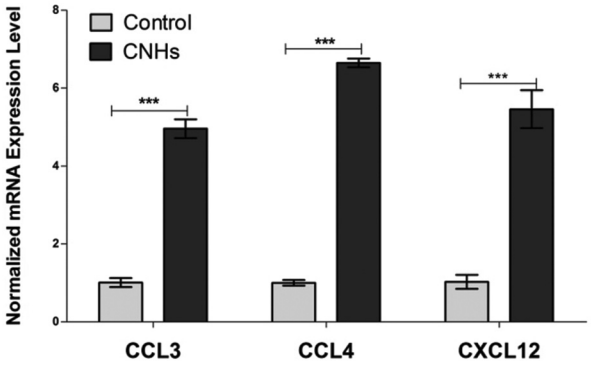

Fig. 4 qPCR analysis of relative expression levels of CCL3, CCL4 CXCL12 cytokines for hMDMs cultured with or without CNHs for 24 hours. ***$p < 0.001$.

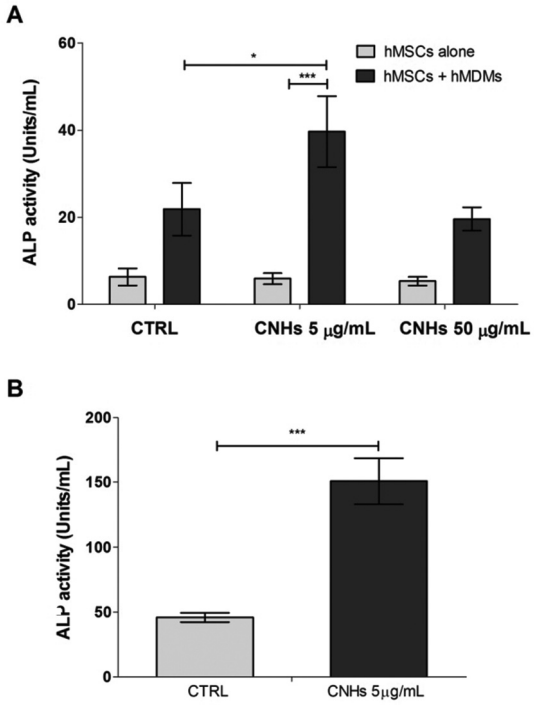

Fig. 5 ALP activity of hMSC alone or cocultured hMDMs and hMSCs with or without CNHs after 7 days (A) and ALP activity cocultured after 14 days (B). ***$p < 0.001$.

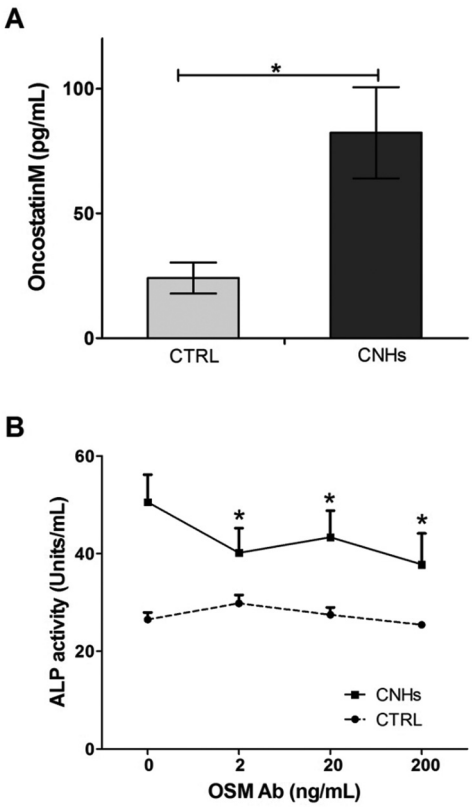

Fig. 6 (A) OSM levels in the supernatants of cocultured hMDMs and hMSCs with or without CNHs. (B) ALP activity was quantified at 7 days after the OSM neutralizing antibody was added to the cocultures with or without CNHs. *$p < 0.05$.

Discussion

In our previous studies, we found that CNHs accelerated bone regeneration. In order to elucidate the mechanism of bone formation, the behavior of macrophages in the presence of CNHs and the effect on mesenchymal stem cells were investigated in cocultured cells.

According to the results of confocal microscopy, a large number of CNHs were located in the hMDMs rather than hMSCs. TEM observations confirmed that CNHs were present in the subcellular compartments of the macrophages (*i.e.* lysosomes and endosomes). It was already reported that phagocytic cells commonly internalize carbon nanohorns *via* endocytosis,[34] and accumulate them in the lysosomes.[35] These results definitely show that CNHs are taken up by macrophages with high selectivity, although the elucidation of the precise process beyond the selective cellular internalization of the CNHs, is an issue of future research.

CNHs did not increase cell apoptosis and necrosis at least up to 50 μg mL^{-1} as shown by flow cytometry analyses, although CNHs were highly accumulated into the lysosomes. Indeed, many researchers have reported that the cytotoxicity of CNHs was very low.[6,29,35,36] However, a high uptake level of CNHs in RAW 264.7, a well-known murine macrophage cell line, seemed to generate reactive oxygen species (ROS), lysosomal membrane destabilization, cell apoptosis and necrosis.[35] Russier *et al.* reported that human macrophages appeared less responsive to carbon nanomaterials in comparison with murine macrophage. This work suggests that hMDMs likely respond to CNHs less than murine macrophage. Our results are similar to those obtained with other types of nanomaterials and nanoparticles, designed for different applications (*i.e.* as contrast agents for imaging or for drug delivery), which resulted immune compatible or could exert

an immune specific action depending on their composition and surface coating.[37,38]

Microarray analysis indicates that chemokine-related genes, including CCL3, CCL4, and CXCL12, were expressed significantly higher in hMDMs treated with CNHs than without CNHs. GO analysis suggests that these up-regulated genes regulate lymphocyte migration. Furthermore, it has been reported that these chemokines are involved not only in immunoregulatory and inflammatory processes but also in tissue repair.[39] For example, CXCL12 was reported to play a role in the maintenance, survival, and osteogenic capacity of immature bone marrow stromal stem cell populations.[40] Our results clearly indicate that CNHs might be promising regulators for a variety of immune system reactions without triggering any cytotoxicity.

In order to elucidate the relation between macrophages with internalized CNHs and bone formation, human macrophage and mesenchymal stem cells were cocultured in the presence of CNHs (Fig. 5). CNHs dramatically increased the ALP activity of the cocultures. According to the TEM observations (Fig. 2C and D), hMDMs have the possibility to communicate with hMSCs *via* molecular signaling because of the tight contact observed between these two types of cells. Several studies have reported that macrophages directly regulate osteogenic differentiation of MSCs through a mechanism that involves cell contact leading to the production of Oncostatin M by monocytes and STAT3 signaling in MSCs.[31,33] OSM, which is produced by activated monocytes, is a multifunctional cytokine that influences the growth and differentiation of several cell types.[32,41] *In vitro* studies on osteoblastic models have demonstrated that OSM stimulates osteogenic differentiation in MSCs [42] and inhibits adipogenic differentiation of hMSCs.[43] In support of these studies, we found that OSM was increased in the medium of cocultured hMSCs and hMDMs. Moreover, OSM was significantly increased in the presence of CNHs (Fig. 6A). An OSM-neutralizing antibody prevented ALP induction in the presence of CNHs but had no effect on ALP activity without CNHs (Fig. 6B). These data suggested that ALP activity is enhanced by OSM produced during coculturing hMDMs and hMSCs in the presence of CNHs.

Even with the addition of an OSM-neutralizing antibody, ALP activity was still higher than control. Therefore there might be other factors involved in the increase of ALP activity. For instance, several studies have reported that CXCL12 promotes the growth, survival, and development of hMSCs,[44] and bone formation.[12,45] Further studies must be performed to find the other factors increasing bone formation by CNHs. However, these data suggested that OSM is one of the possible factors to induce hMSC differentiation into osteoblasts in cocultures with hMDM loaded with CNHs.

The immune cell responses to biomaterial interactions and subsequent effects of factors released by immune cells on osteoblastic cells are important.[46] Few studies with different biomaterials have described bone formation *via* macrophage activation. For example, a recent systematic review of dental implants reported that over 90% of research in this area focused primarily on the *in vitro* behavior of osteoblasts on implant surfaces while only a small percentage (roughly 10%) was dedicated to immune cells.[47] Almost all of the studies about carbon nanomaterials and bone also focused mainly on osteoblasts. For instance, Shimizu *et al.* showed that multi-walled carbon nanotubes (MWCNTs) can promote bone formation by interacting with osteoblasts by accumulating calcium which adhered to MWCNTs.[48] In an *in vitro* study Saito *et al.* found that CNTs are suitable to stimulate osteoblast functions.[49] Misra *et al.* reported that CNHs and graphene oxide inside polymeric materials are able to enhance osteoblast functions and cellular interactions.[13,50] As far as we know, there have been no studies investigating the mechanisms of bone formation using carbon nanomaterials with the focus on the relationship between macrophages, mesenchymal stem cells and these nanomaterials.

This study demonstrates one of the possible mechanisms for bone formation with CNHs. Our findings may be an important milestone and inspire a new design of therapeutic materials for bone regeneration using CNHs such as dental implant and osteoblast cell culture scaffolds.

Experimental section

Preparation of CNH dispersion

CNHs were produced by CO_2 laser ablation of graphite without the metal catalysts.[28] CNHs were oxidized with air by increasing the temperature at 1 °C min^{-1} from room temperature to 500 °C, followed by cooling.[51] Functionalization of CNHs with Alexa488-BSA (Alexa-BSA-CNHs) was performed as previously described.[36] The CNHs or Alexa-BSA-CNHs were dispersed in bovine serum albumin (BSA) at a concentration of 1 mg mL^{-1}. The general medium consisted of DMEM Glutamax media (Gibco) supplemented with 10% heat-inactivated fetal bovine serum (FBS: MP Biomedicals, OH) and streptomycin/penicillin (Gibco). The CNH dispersions by BSA were diluted with the general medium by serial dilution (0.5, 5.0, 50 μg mL^{-1}) and used for human hMDM culture and cocultures of hMDMs and hMSCs.

Cell culture

Ethical approval for the use of peripheral blood from healthy donors was obtained from the Hokkaido University Graduate School of Dental Medicine Ethics Committee (No. 2014-6). Whole blood used in this study was obtained from donors with written informed consent. Peripheral blood mononuclear cells (PBMCs) from healthy adult donors were collected by centrifugation over a Ficoll-Histpaque-1077 (Sigma, MO). $CD14^+$ cells were magnetically labeled with CD14 microbeads and positively selected by MACS Technology (Miltenyi Biotec, Germany). The medium for PBMCs consisted of RPMI 1640 (Sigma) including 10% heat inactivated FBS, 10 mM HEPES (Lonza) and streptomycin/penicillin. PBMCs were cultured at 37 °C, 5% CO_2, in 12-well plates at a density of 3×10^6 cells per well in the medium for PBMC for one day.[52] hMDMs were

obtained by culturing PBMCs in the medium supplemented with 12.5 ng ml^{-1} of a macrophage colony stimulating factor (M-CSF; ImmunoTools) for an additional 6 days. hMSCs were commercially purchased (Product No. PT-2501, Lonza, Switzerland). hMSCs were maintained in a general medium and used between passages 3 and 8. Four hours after seeding, each medium was replaced with the general medium with and without CNHs.

Confocal laser scanning electron microscopy observation

hMSCs were subcultured and stained by the Cell Tracker Red CMPTX dye (Molecular Probes) one day before seeding. Each cell was seeded on an 8-well cell culture slide (Falcon) in 200 μL medium at a density of 5×10^4 cells per mL in the general medium for hMSCs or 5×10^5 cells per mL for hMDMs in the medium for PBMCs. For the cocultures, hMSCs were seeded at first and then hMDMs were seeded on them. Four hours after seeding, each medium was replaced with the medium with and without Alexa-BSA-CNHs (5 μg mL^{-1}). After 24 hours, the cellular uptake of CNHs was observed using an inverted microscope (Nikon Ti-E, Japan) with a confocal laser scanning system (Nikon A1, Japan).

Transmission electron microscopy observation

hMSCs were seeded at first on glass coverslips in 24-well plates at a density of 5000 cells per well and hMDMs were seeded on them at a density of 50 000 cells per well and cultured with and without CNHs (5 μg mL^{-1}) for 24 hours. For TEM samples, polymerized blocks with embedded cells were prepared as previously described.[52] Afterwards, the glass coverslips were removed from the polymerized block surface. A cube-shaped sample was taken from the capsule and a resin was applied to the surface. Then, the cube was laid on its side and cut into ultrathin sections. The ultrathin sections were obtained using an ultramicrotome (Leica) with a diamond knife (DiATOME). The ultrathin sections were examined by TEM (JEM1400 80 V and Titan cubed G2 60-300 operated at 60 kV).

Detection of apoptotic cells

hMDMs were seeded in 98-well plates (1.5×10^5 cells per well) and cultured with each CNH medium (0, 0.5, 5.0, 50 μg mL^{-1}) while DMSO 10% was used as positive control for cell death. Flow cytometry analysis was carried out as previously reported,[52] using APC-Annexin V (AnnV; BD Pharmingen 550475) and propidium iodide (PI, 0.2 μg mL^{-1}; Sigma-Aldrich) in a calcium containing buffer. The percentage of live (AnnV−/PI−), early apoptotic (AnnV+/PI−) and late apoptotic/necrotic (AnnV+/PI+) and AnnV−/PI+) cells was determined by acquiring at least 25 000 events using a FACS Flow Cytometer (Gallios, Beckman Coulter) and by analyzing the data on $CD14^+$ hMDM (FITC-Mouse anti-Human CD14, Clone M5E2, BD Pharmingen 555397) gated populations with FlowJo software.

Microarray analysis

The procedure of DNA microarray analysis has been described in detail previously.[53] Briefly, the total RNA of hMDMs cultured for one day with CNHs (5 μg mL^{-1}) was extracted with ISOGEN (Nippon Gene, Tokyo, Japan) according to the manufacturer's instructions. mRNA was amplified with the Animo Allyl MessageAmp II aRNA amplification kit (Thermo Fisher Scientific, Waltham, MA, USA) and labeled with Cy3 or Cy5. The global gene expression analysis was performed with the Whole Human Genome Microarray Kit 4 × 44 K (Agilent, Santa Clara, CA, USA). The fluorescent intensity of Cy3 and Cy5 in each spot was scanned with a GenePix 4000B and detected with a GenePix Pro (Molecular Devices, Sunnyvale, CA, USA). Gene expression data obtained from fluorescent intensity were globally normalized, and locally weighted scatter plot smoothing adjustment was applied. The DNA microarray experiment was conducted twice, and genes whose expression level ratios from two experiments were less than double were identified as valid data. The extracted up-regulated and down-regulated genes were placed in Gene Ontology bioprocess categories using the PANTHER gene expression analysis/compare gene lists.

Real-time polymerase chain reaction

Total RNA was extracted from one day hMDM cultures using ISOGEN (Nippon gene). First-strand cDNA was synthesized from 500 ng total RNA using Primescript (Takara). The real-time polymerase chain reaction (PCR) contained 10 ng reverse transcribed total RNA, 400 nM primers (Table S1†), and SYBR Premix Ex Taq (Takara). Quantitative PCRs (qPCRs) were carried out on a StepOnePlus RealTime PCR System (Applied Biosystems). Relative quantification was made against serial dilution of GAPDH cDNA which was used as a house-keeping gene.

Measurement of ALP activity

hMSCs were seeded in 24-well plates at a density of 5000 cells per well and hMDMs were seeded on them at a density of 50 000 cells per well for coculture. After 7 and 14 days of cell culture with and without CNHs (0.5, 5, 50 μg mL^{-1}), the amount of the ALP activity in the cells was measured as previously reported.[22]

Measurement of OSM levels and ALP activity with OSM neutralizing antibody

After a 7 day coculture, the OSM levels in supernatants were measured using the Human OSM DuoSet (R&D systems). The OSM neutralizing antibody was added to the cocultures at increasing concentrations (2, 20, 200 ng ml^{-1}) in the general medium and ALP activity was quantified after additional 7 days.

Statistical analysis

All data are presented ± standard error of the mean (SEM). Statistical analyses were performed using GraphPad software

and two-way ANOVA followed by Bonferroni's post-test or Student's *t* test. All *p* values <0.05 were considered significant.

Acknowledgements

E. H. wishes thank the KAKENHI Grant-in-Aid for Young Scientists B (ID No. 26861616). A. Y. wishes to thank the Ministry of Education, Science, Culture and Sport of Japan for Grant-in Aid for Scientific Research B (ID No. 25293389). A. B. wishes to thank JSPS (Japanese Society for the Promotion of Science) for the Invitation Fellowship in Japan (ID No. L15526). E. M. wishes to thank for KAKENHI Grant-in-Aid for Scientific Research (B) (16H03834) and KAKENHI Grant-in-Aid for Challenging Exploratory Research (16K13632). A part of this work was conducted at Hokkaido University, supported by the "Nanotechnology Platform" Program of the Ministry of Education, Culture, Sports, Science and Technology (MEXT), Japan. This work was also partly supported by CNRS. Confocal images were acquired at the Nikon Imaging Center at Hokkaido University.

Notes and references

1 J. J. Li, D. L. Kaplan and H. Zreiqat, *J. Mater. Chem. B*, 2014, **2**, 7272–7306.
2 I. Marangon, C. Ménard-Moyon, A. K. A. Silva, A. Bianco, N. Luciani and F. Gazeau, *Carbon*, 2016, **97**, 110–123.
3 E. Miyako, T. Deguchi, Y. Nakajima, M. Yudasaka, Y. Hagihara, M. Horie, M. Shichiri, Y. Higuchi, F. Yamashita, M. Hashida, Y. Shigeri, Y. Yoshida and S. Iijima, *Proc. Natl. Acad. Sci. U. S. A.*, 2012, **109**, 7523–7528.
4 E. Miyako, K. Kono, E. Yuba, C. Hosokawa, H. Nagai and Y. Hagihara, *Nat. Commun.*, 2012, **3**, 1226.
5 T. Murakami, K. Ajima, J. Miyawaki, M. Yudasaka, S. Iijima and K. Shiba, *Mol. Pharm.*, 2004, **1**, 399–405.
6 J. Wang, Z. Hu, J. Xu and Y. Zhao, *NPG Asia Mater.*, 2014, **6**, e84.
7 K. Yang, L. Feng, X. Shi and Z. Liu, *Chem. Soc. Rev.*, 2013, **42**, 530–547.
8 A. Battigelli, C. Ménard-Moyon and A. Bianco, *J. Mater. Chem. B*, 2014, **2**, 6144–6156.
9 A. Bianco, H. M. Cheng, T. Enoki, Y. Gogotsi, R. H. Hurt, N. Koratkar, T. Kyotani, M. Monthioux, C. R. Park, J. M. D. Tascon and J. Zhang, *Carbon*, 2013, **65**, 1–6.
10 M. Orecchioni, R. Cabizza, A. Bianco and L. G. Delogu, *Theranostics*, 2015, **5**, 710–723.
11 M. Orecchioni, D. A. Jasim, M. Pescatori, R. Manetti, C. Fozza, F. Sgarrella, D. Bedognetti, A. Bianco, K. Kostarelos and L. G. Delogu, *Adv. Healthcare Mater.*, 2016, **5**, 276–287.
12 P. A. Tran, L. Zhang and T. J. Webster, *Adv. Drug Delivery Rev.*, 2009, **61**, 1097–1114.
13 R. D. K. Misra and P. M. Chaudhari, *J. Biomed. Mater. Res., Part A*, 2013, **101 A**, 528–536.
14 D. Depan and R. D. K. Misra, *Nanoscale*, 2012, **4**, 6325–6335.
15 R. D. K. Misra, D. Depan and J. S. Shah, *Acta Biomater.*, 2012, **8**, 1908–1917.
16 R. D. K. Misra and Q. Yuan, *Mater. Sci. Eng., C*, 2012, **32**, 902–908.
17 B. Girase, J. S. Shah and R. D. K. Misra, *Adv. Eng. Mater.*, 2012, **14**, 101–111.
18 R. D. K. Misra, B. Girase, D. Depan and J. S. Shah, *Adv. Eng. Mater.*, 2012, **14**, 93–100.
19 E. Hirata, T. Akasaka, M. Uo, H. Takita, F. Watari and A. Yokoyama, *Appl. Surf. Sci.*, 2012, **262**, 24–27.
20 E. Hirata, M. Uo, Y. Nodasaka, H. Takita, N. Ushijima, T. Akasaka, F. Watari and A. Yokoyama, *J. Biomed. Mater. Res., Part B*, 2010, **93**, 544–550.
21 E. Hirata, M. Uo, H. Takita, T. Akasaka, F. Watari and A. Yokoyama, *J. Biomed. Mater. Res., Part B*, 2009, **90**, 629–634.
22 E. Hirata, M. Uo, H. Takita, T. Akasaka, F. Watari and A. Yokoyama, *Carbon*, 2011, **49**, 3284–3291.
23 C. A. Poland, R. Duffin, I. Kinloch, A. Maynard, W. A. H. Wallace, A. Seaton, V. Stone, S. Brown, W. Macnee and K. Donaldson, *Nat. Nanotechnol.*, 2008, **3**, 423–428.
24 K. Kostarelos, *Nat. Biotechnol.*, 2008, **26**, 774–776.
25 T. Kasai, S. Matsumura, T. Iizuka, K. Shiba, T. Kanamori, M. Yudasaka, S. Iijima and A. Yokoyama, *Nanotechnology*, 2011, **22**, 065102.
26 D. Depan and R. D. K. Misra, *Acta Biomater.*, 2013, **9**, 6084–6094.
27 T. Murakami, H. Sawada, G. Tamura, M. Yudasaka, S. Iijima and K. Tsuchida, *Nanomedicine*, 2008, **3**, 453–463.
28 S. Iijima, M. Yudasaka, R. Yamada, S. Bandow, K. Suenaga, F. Kokai and K. Takahashi, *Chem. Phys. Lett.*, 1999, **309**, 165–170.
29 J. Miyawaki, M. Yudasaka, T. Azami, Y. Kubo and S. Iijima, *ACS Nano*, 2008, **2**, 213–226.
30 R. J. Miron and D. D. Bosshardt, *Biomaterials*, 2016, **82**, 1–19.
31 V. Nicolaidou, M. M. Wong, A. N. Redpath, A. Ersek, D. F. Baban, L. M. Williams, A. P. Cope and N. J. Horwood, *PLoS One*, 2012, **7**, e39871.
32 M. J. Gómez-Lechón, *Life Sci.*, 1999, **65**, 2019–2030.
33 P. Guihard, Y. Danger, B. Brounais, E. David, R. Brion, J. Delecrin, C. D. Richards, S. Chevalier, F. Rédini, D. Heymann, H. Gascan and F. Blanchard, *Stem Cells*, 2012, **30**, 762–772.
34 S. Lacotte, A. García, M. Décossas, W. T. Al-Jamal, S. Li, K. Kostarelos, S. Muller, M. Prato, H. Dumortier and A. Bianco, *Adv. Mater.*, 2008, **20**, 2421–2426.
35 Y. Tahara, M. Nakamura, M. Yang, M. Zhang, S. Iijima and M. Yudasaka, *Biomaterials*, 2012, **33**, 2762–2769.
36 M. Horie, L. K. Komaba, H. Fukui, H. Kato, S. Endoh, A. Nakamura, A. Miyauchi, J. Maru, E. Miyako, K. Fujita, Y. Hagihara, Y. Yoshida and H. Iwahashi, *Carbon*, 2013, **54**, 155–167.

37 S. Dolci, V. Domenici, G. Vidili, M. Orecchioni, P. Bandiera, R. Madeddu, C. Farace, M. Peana, M. R. Tiné, R. Manetti, F. Sgarrella and L. G. Delogu, *RSC Adv.*, 2016, **6**, 2712–2723.

38 C. Farace, P. Sánchez-Moreno, M. Orecchioni, R. Manetti, F. Sgarrella, Y. Asara, J. M. Peula-García, J. A. Marchal, R. Madeddu and L. G. Delogu, *Sci. Rep.*, 2016, **6**, 18423–18437.

39 R. Gillitzer and M. Goebeler, *J. Leukocyte Biol.*, 2001, **69**, 513–521.

40 A. Kortesidis, A. Zannettino, S. Isenmann, S. Shi, T. Lapidot and S. Gronthos, *Blood*, 2005, **105**, 3793–3801.

41 M. Tanaka and A. Miyajima, *Rev. Physiol., Biochem. Pharmacol.*, 2003, **149**, 39–52.

42 C. Chipoy, M. Berreur, S. Couillaud, G. Pradal, F. Vallette, C. Colombeix, F. Rédini, D. Heymann and F. Blanchard, *J. Bone Miner. Res.*, 2004, **19**, 1850–1861.

43 H. Y. Song, E. S. Jeon, J. Il Kim, J. S. Jung and J. H. Kim, *J. Cell. Biochem.*, 2007, **101**, 1238–1251.

44 T. Kitaori, H. Ito, E. M. Schwarz, R. Tsutsumi, H. Yoshitomi, S. Oishi, M. Nakano, N. Fujii, T. Nagasawa and T. Nakamura, *Arthritis Rheum.*, 2009, **60**, 813–823.

45 S. Otsuru, K. Tamai, T. Yamazaki, H. Yoshikawa and Y. Kaneda, *Stem Cells*, 2008, **26**, 223–234.

46 Q.-L. Ma, L.-Z. Zhao, R.-R. Liu, B.-Q. Jin, W. Song, Y. Wang, Y.-S. Zhang, L.-H. Chen and Y.-M. Zhang, *Biomaterials*, 2014, **35**, 9853–9867.

47 G. Thalji and L. F. Cooper, *Int. J. Oral Maxillofac. Implants*, 2014, **29**, e171–e199.

48 M. Shimizu, Y. Kobayashi, T. Mizoguchi, H. Nakamura, I. Kawahara, N. Narita, Y. Usui, K. Aoki, K. Hara, H. Haniu, N. Ogihara, N. Ishigaki, K. Nakamura, H. Kato, M. Kawakubo, Y. Dohi, S. Taruta, Y. A. Kim, M. Endo, H. Ozawa, N. Udagawa, N. Takahashi and N. Saito, *Adv. Mater.*, 2012, **24**, 2176–2185.

49 N. Saito, Y. Usui, K. Aoki, N. Narita, M. Shimizu, N. Ogiwara, K. Nakamura, N. Ishigaki, H. Kato, S. Taruta and M. Endo, *Curr. Med. Chem.*, 2008, **15**, 523–527.

50 R. D. K. Misra and P. M. Chaudhari, *J. Biomed. Mater. Res., Part A*, 2013, **101 A**, 1059–1068.

51 J. Fan, M. Yudasaka, J. Miyawaki, K. Ajima, K. Murata and S. Iijima, *J. Phys. Chem. B*, 2006, **110**, 1587–1591.

52 J. Russier, E. Treossi, A. Scarsi, F. Perrozzi, H. Dumortier, L. Ottaviano, M. Meneghetti, V. Palermo and A. Bianco, *Nanoscale*, 2013, **5**, 11234–11247.

53 N. Hanagata, F. Zhuang, S. Connolly, J. Li, N. Ogawa and M. Xu, *ACS Nano*, 2011, **5**, 9326–9338.